© 2017

Crystallization of Anatase TiO$_2$ in Niobium Potassium Phosphate Glasses

Carolina Dakuzaku Freschi[a], José Tadeu Gouveia[a], Lia Marcondes[a], Jefferson Luis Ferrari[b], Fábia

Castro Cassanjes[a], Gael Poirier[a]*

[a] Research Group of Materials Chemistry, Universidade Federal de Alfenas, Campus de Poços de Caldas, Poços de Caldas, MG, Brazil
[b] Departamento de Ciências Naturais, Universidade Federal de São João Del Rei, Campus Dom Bosco, Praça Dom Helvécio, 74, CEP 36301-160, São João Del Rei, MG, Brazil

In this work, the glass forming ability was studied in potassium phosphate glasses with increasing amounts of TiO$_2$ in order to obtain a glass-ceramic with photocatalytic properties. The first studied series has been the binary system (100-x) KPO$_3$-xTiO$_2$. Homogeneous and transparent glasses could be obtained with x varying from 10 to 30 mole%. Since the photocatalytic anatase phase could not be precipitated in this system, the ternary system KPO$_3$-TiO$_2$-Nb$_2$O$_5$ was investigated in order to incorporate higher TiO$_2$ contents without spontaneous crystallization under cooling. Thermal properties of all glass samples were investigated by DSC and allowed identifying an increase of glass transition temperatures with increasing TiO$_2$. For all compositions, exothermic events related with crystallization were also observed and suitable heat-treatments resulted in specific crystalline phases identified by X-ray diffraction. Selective precipitation of the anatase titanium oxide was successfully obtained from the glass compostion 35KPO$_3$-25Nb$_2$O$_5$-40TiO$_2$ (KN25T40) after heat treatment at 720°C for 2 h, suggesting the possibility of obtaining a glass-ceramic for photocatalytic applications. Structural investigations by Raman were also performed on glasses and glass-ceramics and allowed to point out the glass intermediary behavior of TiO$_2$ in the phosphate vitreous network where TiO$_4$ and TiO$_6$ octahedra are inserted inside the phosphate network with TiO$_6$ clusters identified at higher TiO$_2$ contents. Raman analysis also identified anatase TiO$_2$ in the KN25T40 glass-ceramic.

Keywords: *glass; phosphate; titanium oxide; anatase*

1. Introduction

Titanium dioxide is considered one of the most important semiconductor oxide with interesting chemical, electrical and optical properties. Since its discovery as photocatalytic agent observed by Fujishima and Honda in 1972, research on TiO$_2$ applications has attracting considerable interest in several fields of science due to its excellent properties, including chemical stability, photostability and appropriate electronic band structure[1,2].

Titanium dioxide thin films have been formed on glass, steel and other surfaces by a wide range of techniques, especially by sol-gel and chemical vapour deposition[3,4]. However, the properties of these materials produced by deposition or coating techniques can change over time by surface damage and thus a recoating process can be necessary. On the other hand, TiO$_2$ crystallites precipitated in the glass matrix can exhibit stable physical and chemical properties even with surface polishing[5].

There are three allotropic forms of TiO$_2$: anatase (tetragonal), brookite (orthorhombic) and rutile (tetragonal) among which rutile is the most thermodynamically stable

phase for bulk TiO$_2$ under most conditions. However, the rutile activity as a photocatalytic compound is generally poor. Anatase TiO$_2$ is considered to be the active photocatalytic component based on charge carrier dynamics, chemical properties and the activity of photocatalytic degradation of organic compounds[1,3].

When a glass-ceramic is obtained by heat-treatment of the mother glass, both the disordered glass regions and ordered crystalline regions are presents. The final material can exhibit not only the benefits of the glass material but also the unique physical properties originated from the crystalline phase. However, only a few works reported phosphate glass-ceramics containing anatase TiO$_2$ in crystal volume fraction by heat treatment and this lack is in part attributed to the difficulty of promoting controlled and selective crystallization of anatase in phosphate-based glasses with high TiO$_2$ contents since titania is known to act as a nucleating agent of other crystalline phases[6].

Selective crystallization of the glass CaO-Bi$_2$O$_3$-B$_2$O$_3$-Al$_2$O$_3$-TiO$_2$ containing 20% TiO$_2$ under heat-treatment using an infrared halogen lamp is reported but allowed only precipitation of the rutile phase[7]. Recently, selective crystallization of TiO$_2$ by controlled heat-treatment and SiO$_2$

addition in the glass 14TiO$_2$-23ZnO-45B$_2$O$_3$-18Al$_2$O$_3$ was also reported[8] but XRD results indicate that TiO$_2$ was not the unique crystalline phase after heat treatment and Al$_4$B$_2$O$_9$ was precipitated as a subcrystalline phase.

In this work, TiO$_2$-containing glass compositions were investigated for preferential anatase crystallization. First, the binary system (100-x)KPO$_3$-xTiO$_2$ was investigated and glass samples were obtained from x=10 to x=30. These glasses were characterized by DSC and Raman spectroscopy and specific heat-treatments were performed but anatase could not be precipitated under heat-treatments. Adding Nb$_2$O$_5$ to this binary system allowed incorporating higher TiO$_2$ contents (40%) and anatase TiO$_2$ could be successfully precipitated in the mother glass.

2. Experimental Part

Glass samples were synthesized from the precursors: titanium dioxide 99,9% (TiO$_2$) from Vetec, potassium phosphate monobasic 99,9% (KH$_2$PO$_4$) from Synth and niobium oxide 99,8% (Nb$_2$O$_5$) from Sigma-Aldrich by conventional melt-quenching: The starting powders were weighted using an analytical balance and grinded in an agate mortar. The batches were melted for 2 hours in a platinum crucible between 1100 and 1450°C depending on the TiO$_2$ content. Finally, the melts were quenched in a steel mold preheated 20°C below the glass transition temperature and kept at this temperature for 8 hours before slow cooling inside the furnace.First, samples in the binary system (100-x) KPO$_3$-xTiO$_2$ with x varying from 10 to 30 (mole%) were prepared using the methodology described above. In a second step, a ternary system was investigated with the introduction of niobium oxide as glass intermediary in order to increase the TiO$_2$ content in the final glass using the same methodology. Molar compositions, melting temperature and visual aspect of the glass samples are presented in Table 1. DSC curves were performed on bulk glass samples of 30 mg in Pt/Rh covered crucibles between 200°C and 1100°C at 10°C/min under N$_2$ atmosphere. These thermal analyzes were obtained using a DSC/TG calorimeter STA 449 F3 Jupiter from Netzsch. X-ray diffraction measurements were performed on powder samples using a Rigaku ultima

IV diffractometer working at 40KV and 30mA between 10º and 70º in continuous mode of 0,02º/s. The crystalline phases were identified according to X-ray powder diffraction patterns (PDF file)[9]. Finally, Raman spectra were collected on bulk glass samples between 100cm^{-1} and 1200cm^{-1} using a LabRam Micro-Raman from Horiba Jobin-Yvon operating at 632,8 nm with a He-Ne laser.

3. Results

Transparent and homogeneous samples were obtained in the binary system (100-x)KPO$_3$ - xTiO$_2$ with x varying from 10 to 30 mole% by melt-quenching with an increasing brownish color for higher TiO$_2$ contents. As expected, an increase of the melt viscosity with increasing TiO$_2$ content was observed during synthesis and higher melting temperatures were used for a suitable casting of the melt. However, partial or total crystallization of the samples was observed for TiO$_2$ contents above 30 mole% under these experimental conditions. After X-ray diffraction analysis of the crystalline phases obtained by heat-treatment in these glasses, Nb$_2$O$_5$ was added and samples containing 40 mole% of TiO$_2$ could be prepared. In fact, several compositions were tested by varying the KPO$_3$:Nb$_2$O$_5$ ratio (50:10; 40:20; 35:25; 30:30) with constant TiO$_2$ content of 40%. Compositions 50KPO$_3$-10Nb$_2$O$_5$-40TiO$_2$ and 30KPO$_3$-30Nb$_2$O$_5$-40TiO$_2$ crystallized under quenching while compositions 40KPO$_3$-20Nb$_2$O$_5$-40TiO$_2$ and 35KPO$_3$-25Nb$_2$O$_5$-40TiO$_2$ sucessfully vitrified. Table 1 resumes all investigated compositions, required melting temperatures and the visual aspect of the final samples. DSC curves for all bulk glass samples are presented in Figure 1 and Table 2 resumes the characteristic temperatures Tg, Tx and Tf where Tg is the glass transition temperature, Tx the onset of crystallization and Tf the melting temperature as well as the thermal stability parameter Tx-Tg. These thermal data point out that the addition of TiO$_2$ results in a significant increase in Tg values from 330°C to 510°C in the binary system KPO$_3$-TiO$_2$ with an increase of the thermal stability parameter from 10% to 20% and further decrease for higher contents. Nb$_2$O$_5$ incorporation also results in a clear increase of Tg identified around 650°C for 20 and 25 mole% of niobium oxide. Crystallization events were

Table 1. Molar compositions, characteristic temperatures and visual aspect of the glass samples.

Sample	Molar Compositions (% mol)			Melting Temperature (°C)	Picture
	KPO$_3$	TiO$_2$	Nb$_2$O$_5$		
KT10	90	10	___	1100	
KT20	80	20	___	1200	
KT30	70	30	___	1300	
KN25T40	35	40	25	1450	
KN20T40	40	40	20	1500	
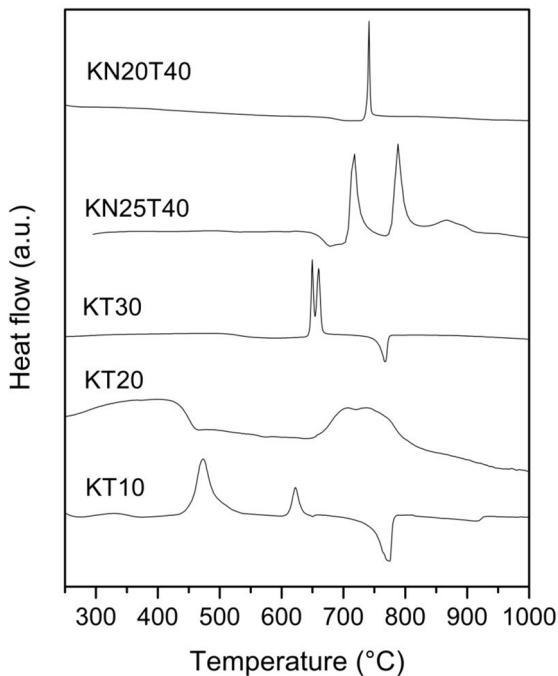
Figure 1. DSC curves of glass samples in the binary system KPO_3-TiO_2 (10-30% TiO_2) and ternary KPO_3-Nb_2O_5-TiO_2 (40% TiO_2).

observed for all samples as well as melting for glasses KT10 and KT30 at the same temperature. Heat-treatments were applied near the crystallization temperatures in order to identify the crystallization events observed by DSC and check the ability of these glass compositions to precipitate titanium dioxide crystalline phases and especially anatase, which is known for its efficient photocatalytic properties. The crystalline phase identifications performed by X-ray diffraction are summarized in Figure 2 and Figure 3 as well as Table 2. Sample KT10 only exhibited precipitation of long-chains potassium metaphosphate KPO_3 whereas sample KT20 suffered crystallization of potassium pyrophosphate

$K_4P_2O_7$ and cyclic potassium metaphosphate $K_3P_3O_9$. For sample KT30, phases KPO_3 and $KTiOPO_4$ were detected. Finally, for samples modified with niobium oxide, anatase TiO_2 could be identified as the first precipitated phase in sample KN25T40 heat-treated below the first crystallization peak whereas heat-treatments at higher temperatures induce crystallization of the mother glass with formation of $K_2TiNb_2P_2O_{13}$. For the other niobium titanium phosphate glass KN20T40, crystalline phases $K_2TiNb_2P_2O_{13}$, $K_3Nb_6P_4O_{26}$ and rutile TiO_2 were identified.

Raman spectra of the glass samples and crystalline references KPO_3, TiO_2 and Nb_2O_5 in the frequency region between 100 and 1500 cm^{-1} were recorded to probe the structural evolution with TiO_2 addition and to compare the Raman features of precursor glass and glass-ceramic KN25T40 (Figure 4). In the binary system KPO_3-TiO_2, the first clear change in Raman spectra is the progressive vanishing of vibrational bands centered at 1150cm^{-1} and 680cm^{-1} and commonly attributed to symmetric stretching modes of P-O bonds in P-O-P linkages and Q^2 tetrahedra in metaphosphate compounds[10-11]. On the other hand, TiO_2 addition results in new Raman signals centered around 1250cm^{-1} and 520cm^{-1} which shifts to lower wavenumbers. These signals are reported to be due to P=O terminal bonds in PO_4 tetrahedra wherein the other three oxygens are linked to another cation (P-O-X where X=P or Ti) and vibrational modes of distorted TiO_6 respectively[10]. Other Raman features appear with TiO_2 addition at 290cm^{-1}, 735cm^{-1}, 863cm^{-1}, 935cm^{-1} and 977cm^{-1} and were attributed to bending modes of TiO_6 octahedra[12], stretching modes of TiO_6[10,13], stretching modes of TiO_4[14-15], Ti-O stretchings of the axial Ti-O bond in TiO_5 pyramidal units[10,16-17] and PO_4 orthophosphate units respectively[18]. Precursor glass composition KN25T40 is dominated by broad Raman bands centered around 200 cm^{-1}, 650 cm^{-1} and 825 cm^{-1} as for crystalline Nb_2O_5 whereas the glass-ceramic exhibits sharper Raman signals at 240 cm^{-1} and 640 cm^{-1} as for crystalline anatase TiO_2.

Table 2. Characteristic temperatures, thermal stability and crystalline phases identified in heat-treated glass samples.

Samples	Characteristic temperatures (°C)					Thermal stability parameter	Crystalline phase after heat-treatments
	Tg	Tx_1	Tx_2	Tx_3	Tf	Tx_1-Tg	
KT10	330	475	620	-	780	145	KPO_3
KT20	440	705	740	-	-	265	$K_4P_2O_7$ $K_3P_3O_9$
KT30	510	650	660	-	770	140	KPO_3 $KTiOPO_4$
KN20T40	670	730	-	-	-	60	Rutile TiO_2 $K_3Nb_6P_4O_{26}$ $K_2TiNb_2P_2O_{13}$
KN25T40	650	720	790	870		70	Anatase TiO_2 $K_2TiNb_2P_2O_{13}$

- Event not observed.
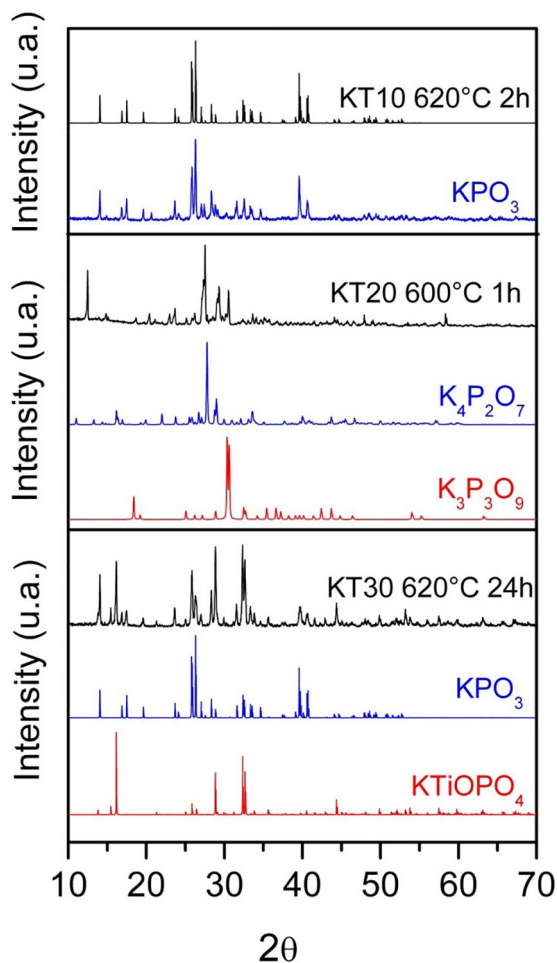
Figure 2. X-ray diffraction patterns of heat-treated glasses in the binary system KPO$_3$-TiO$_2$.

Figure 3. X-ray diffraction patterns of heat-treated glasses in the ternary system KPO$_3$-Nb$_2$O$_5$-TiO$_2$.

4. Discussion

Since the main objective of this work was the obtaining of glass-ceramics containing anatase crystallites for photocatalytic applications, the glass forming ability of the binary system KPO$_3$-TiO$_2$ was investigated with increasing amounts of TiO$_2$. Homogeneous glass samples were obtained by melt-quenching from TiO$_2$ contents ranging from 10 to 30 mole% whereas higher contents lead to crystallized samples under these experimental conditions. As presented in Table 1, these glasses also exhibit an increasing brownish color attributed to partial titanium reduction from Ti^{4+} to Ti^{3+}. It is suggested that the increasing melting temperatures can induce oxygen loss of the melt and titanium reduction as described for non-stochiometric crystalline titanium oxides. The strong absorption in the visible is due to both d-d internal electronic transition of Ti^{3+} (d^1 electronic configuration) and electronic polaron transitions between reduced Ti^{3+} and oxidized Ti^{4+} species[19-20]. These increasing melting temperatures and increasing viscosity of the resulting melt observed during synthesis bring a first indication of the effective insertion of
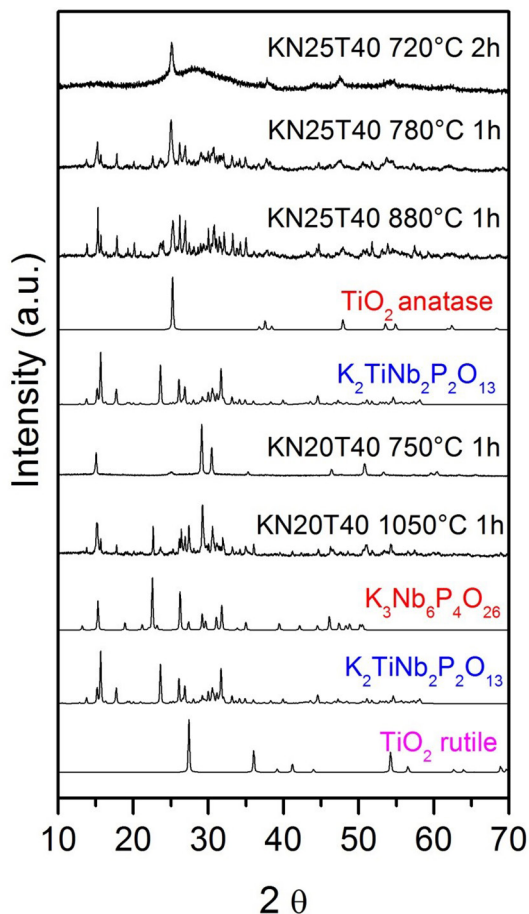
titanium ions inside the phosphate chains and higher network connectivity and field strength. A detailed structural description can be extracted from a general analysis of thermal results, Raman data and crystalline phase identification obtained by X-ray diffraction. Since the results obtained from each technique point out the same structural evolution, these data are discussed simultaneously. The first important point is the clear increase of glass transition temperatures from 330ºC to 510ºC for TiO$_2$ contents ranging from 10 to 30 mole%. This behavior is commonly related with an increase in the glass network connectivity as well as in the network bond strength as reported in many structural studies concerning transition metal oxide-containing phosphate glasses. In fact, these metallic oxides usually exhibit strong metal-oxygen bonds and high coordination number. In addition, their intermediary behavior in phosphate network usually allow their partial or complete insertion inside the phosphate covalent chains, resulting in cross-linking bonds between these chains. In our case, the Tg increase with composition can be attributed to a progressive insertion of titanium oxide units such as TiO$_4$ and/or TiO$_6$ between PO$_4$ tetrahedra. These species were identified by the Raman bands observed at 863cm^{-1}
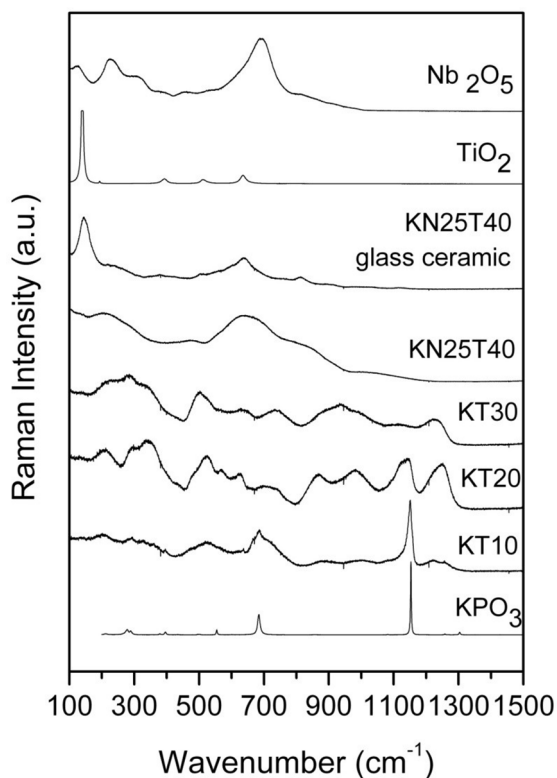
Figure 4. Raman spectra of glasses, glass-ceramic KN25T40 and crystalline references TiO_2, Nb_2O_5 and KPO_3.

and 520cm⁻¹ respectively. The former Raman band is often attributed to Nb-O-P linkages[21] but is better attributed to TiO_4 units in these glasses since niobium free samples prepared in the binary system KPO_3-TiO_2 also exhibit this signal. The potassium metaphosphate network depolymerisation is also supported by the progressive vanishing of Raman bands at 680cm⁻¹ and 1150cm⁻¹ related with P-O-P and P-O terminal bonds in Q^2 tetrahedra. Another important result supporting this structural evolution is the preferential precipitation of potassium metaphosphate KPO_3 in sample KT10 at 475ºC which melts at 780ºC whereas sample KT20 exhibits crystallization of potassium pyrophosphate $K_4P_2O_7$ and cyclic metaphosphate $K_3P_3O_9$. The other crystallization event observed for KT10 can be related with precipitation of titanium oxide with high melting temperature not observed below 1000ºC. These titanium oxide polyhedra can increase the network connectivity by cross-linked Ti-O-P bonds. In fact, the appearance of the Raman band around 1250cm⁻¹ and attributed to P=O bonds means that all other P-O linkages in these PO_4 tetrahedra are bridging bonds like P-O-Ti bonds resulting in this non-resonant P=O species. Based on the well-known glass intermediary behavior of Nb_2O_5 in phosphate glasses, it is also suggested that niobium oxide incorporation promotes bridging Nb-O-P bonds and higher glass network connectivity, in agreement with higher Tg temperatures for these glasses. In addition, The Raman band

centered at 863cm⁻¹ and attributed to TiO_4 units enhances from 10% to 20% of TiO_2 but further decreases for 30% but a new band at 935cm⁻¹ clearly appears for KT30. Since this Raman signal is known to be due to the axial Ti-O bond in pyramidal TiO_5 units, it can be suggested that titanium ions are preferentially four-fold and six-fold coordinated for lower TiO_2 contents whereas TiO_6 and TiO_5 units dominate for higher titanium oxide concentrations. The precipitation of titanium-containing crystalline phases could not be detected by X-ray diffraction of the heat-treated samples KT10 and KT20 but the thermal behavior of sample KT30 also gives important structural clues explaining the limited glass forming ability of this binary system. The Raman spectrum of this sample is dominated by signals centered at 290, 520, 935 and 1250cm⁻¹ related with TiO_6, TiO_5 and PO_4 units whereas the DSC curve exhibits two crystallization peaks and a melting event. Heat-treatment of this sample resulted in precipitation of crystalline phases KPO_3 and $KTiOPO_4$. Since the Tg temperature of this glass is higher than compositions KT10 and KT20, it appears that titanium oxide polyhedra effectively modified the phosphate network through P-O-Ti bonds but the thermal treatment induces a spontaneous phase separation of a potassium metaphosphate structure and potassium titanium orthophosphate constituted of TiO_6 octahedra and orthophosphate PO_4^{3-} ions. The KPO_3 formation has been detected by X-ray diffraction as well as melting event observed at 770ºC. This phase separation tendency for these higher TiO_2 contents is in agreement with the spontaneous crystallization of melts with higher TiO_2 contents by melt-quenching.

Anyway, these binary compositions were not able to precipitate TiO_2 anatase by heat-treatment and niobium oxide Nb_2O_5 was added in order to investigate the glass forming ability of compositions with 40 mole% of TiO_2. Samples with 10% and 30% of Nb_2O_5 crystallized under quenching while compositions with 20% and 25% successfully vitrified (KN20T40 and KN25T40). For sample KN20T40, only one crystallization peak was observed by DSC with Tx at 730ºC and heat-treatments were performed at 750ºC and 1050ºC in order to identify the first crystalline phase as well as other possible precipitations not detected by thermal analysis. The first heat-treatment resulted in a diffraction pattern that could not be identified using the ICSD database whereas heat-treatment at higher temperatures allowed characterizing the potassium niobium phosphate $K_3Nb_6P_4O_{26}$, potassium niobium titanium phosphate $K_2TiNb_2P_2O_{13}$ and rutile TiO_2. For this composition, these results clearly point out that these crystalline phase precipitation are not related with distinct crystallization peaks and can hardly be selectively precipitated by suitable heat-treatments. The chemical composition of these phases suggests crystallization of the mother glass with rutile TiO_2. In any case, anatase TiO_2 could not be detected for this composition. On the other hand, sample KN25T40 exhibits three distinct exothermic

events starting at 720ºC, 790ºC and 870ºC attributed to precipitation of several crystalline phases in the glass. For this reason, heat-treatments were performed at 720ºC, 780ºC and 880ºC and the resulting samples were characterized by X-ray diffraction. As shown in Figure 3 and Table 2, these results allowed attributing the first peak to precipitation of anatase while the second exothermic event is related with crystallization of $K_2TiNb_2P_2O_{13}$. A stoichiometric analysis of the starting glass composition ($35KPO_3$-$25Nb_2O_5$-$40TiO_2$ corresponding to $K_7Ti_8Nb_{10}P_7O_{62}$ average formula) and final crystalline phases TiO_2 and $K_2TiNb_2P_2O_{13}$ suggest that approximately half of the starting titanium ions is precipitated as anatase resulting in a final composition of the residual glass next to $K_7Ti_4Nb_{10}P_7O_{54}$ which is close to the composition of the crystalline phase $K_2TiNb_2P_2O_{13}$. For this composition, it has been shown that anatase can be preferentially precipitated as the first crystalline phase in these glasses resulting in a glass-ceramic containing only anatase crystallites. The Raman data presented in Figure 4 also support this assumption. The Raman spectrum of the precursor glass KN25T40 exhibits intense signals around $230cm^{-1}$, $750cm^{-1}$ and $850cm^{-1}$ also observed for crystalline Nb_2O_5 and attributed to bending and stretching modes of NbO_6 octahedra. The higher polarizability of Nb-O bonds when compared to P-O and Ti-O bonds explains why the former bonds dominate the spectrum when compared to the latter one. On the other hand, The Raman spectrum of the glass-ceramic KN25T40 obtained from heat-treatment of the starting glass at 720ºC shows a very distinct signal with dominant narrow bands centered at $150cm^{-1}$ and $650cm^{-1}$ characteristic of bending and stretching modes of the crystalline phase anatase.

5. Conclusion

Homogeneous and transparent titanophosphate glasses were obtained in the binary KPO_3-TiO_2 and ternary KPO_3-TiO_2-Nb_2O_5 systems by the melt-quenching method. 30 mole% of TiO_2 was successfully incorporated without devitrification in the binary system and the structural changes were monitored by DSC, Raman and X-ray diffraction of the heat-treated glasses. Titanium oxide polyhedra are inserted inside the phosphate chains and increase the network connectivity. However, for higher TiO_2 contents, a phase separation has been identified without precipitation of the desired anatase TiO_2 phase. Addition of Nb_2O_5 as an intermediary compound led to important structural changes, increasing the stability against devitrification and homogeneous glasses containing 40% TiO_2 could be obtained. The glass composition $35KPO_3$-$25Nb_2O_5$-$40TiO_2$ exhibits a preferential precipitation of anatase in the mother glass resulting in glass-ceramics with a potential photocatalytic activity.

6. Acknowledgments

7. References

1. Ye M, Vennerberg D, Lin C, Lin Z. Nanostructured TiO₂ architectures for environmental and energy applications. *Journal of Nanoscience Letters*. 2012;2:1-35.

2. Fujishima A, Honda K. Electrochemical photolysis of water at a semiconductor electrode. *Nature*. 1972;238(5358):37-38.

3. Gupta SM, Tripathi M. A review of TiO₂ nanoparticles *Chinese Science Bulletin*. 2011;56:1639-1657.

4. Page K, Palgrave RG, Parkin IP, Wilson M, Savin SLP, Chadwick AV. Titania and silver-titania composite films on glass-potent antimicrobial coatings. *Journal of Materials Chemistry*. 2007;17(1):95-104.

5. Yazawa T, Machida F, Oki K, Mineshige A, Kobune M. Novel porous TiO₂ glass-ceramics with highly photocatalytic ability. *Ceramics International*. 2009;35(4):1693-1697.

6. Masai H, Fujiwara T, Mori H, Komatsu T. Fabrication of TiO₂ nanocrystallized glass. *Applied Physics Letters*. 2007;90(8):081907.

7. Masai H, Kanamori E, Takahashi Y, Fujiwara T. Surface crystallization of CaO–Bi₂O₃–B₂O₃–Al₂O₃–TiO₂ glass using IR furnace. *Journal of Non-Crystalline Solids*. 2010;356(52-54):2977-2979.

8. Yoshida K, Masai H, Takahashi Y, Ihara R, Fujiwara T. Selective crystallization of anatase and rutile by control of heat-treatment conditions and SiO₂ addition in TiO₂-crystallized glass. *Journal of the Ceramic Society of Japan*. 2013;121(1420):999-1003.

9. International Centre for Diffraction Data-Joint Committee of Powder Diffraction Standards. *Powder diffraction file (PDF)*. Newton Square: International Centre for Diffraction Data-Joint Committee of Powder Diffraction Standards; 2000.

10. Cardinal T, Fargin E, Flem E, Couzi M. Raman Scattering and XAFS Study of Optically Nonlinear Glasses of the TiO₂-NaPO₃-Na₂B₄O₇ System. *Journal of Solid State Chemistry*. 1995;120(1):151-156.

11. Kaur M, Singh A, Thakur V, Singh L. Effect of TiO₂ substitution on optical and structural aspects of phosphate glasses. *Journal of Molecular Structure*. 2015;1089:95-101.

12. Farrow LA, Vogel EM. Raman spectra of phosphate and silicate glasses doped with the cations Ti, Nb and Bi. *Journal of Non-Crystalline Solids*. 1992;143:59-64.

13. Dias AG, Skakle JMS, Gibson IR, Lopes MA, Santos JD. In situ thermal and structural characterization of bioactive calcium phosphate glass ceramics containing TiO₂ and MgO oxides: High temperature – XRD studies. *Journal of Non-Crystalline Solids*. 2005;351(10-11):810-817.

14. Sakka S, Miyaji F, Fukumi K. Structure of binary K₂O-TiO₂ and Cs₂O-TiO₂ glasses. *Journal of Non-Crystalline Solids*. 1989;112(1-3):64-68.

15. Zheng K, Liao J, Wang X, Zhang Z. Raman spectroscopic study of the structural properties of CaO–MgO–SiO2–TiO2 slags. *Journal of Non-Crystalline Solids*. 2013;376:209-215.

16. Magyari K, Stefan R, Vulpoi A, Baia L. Bioactivity evolution of calcium-free borophosphate glass with addition of titanium dioxide. *Journal of Non-Crystalline Solids*. 2015;410:112-117.

17. Tiwari B, Pandey M, Sudarsan V, Deb SK, Kothiyal GP. Study of structural modification of sodium aluminophosphate glasses with TiO$_2$ addition through Raman and NMR spectroscopy. *Physica B: Condensed Matter*. 2009;404(1):47-51.

18. Morikawa H, Lee S, Kasuga T, Brauer DS. Effects of magnesium for calcium substitution in P$_2$O$_5$–CaO–TiO$_2$ glasses. *Journal of Non-Crystalline Solids*. 2013;380:53-59.

19. El Batal FH, Ibrahim S, Marzouk MA. UV–visible, infrared absorption spectra of undoped and TiO$_2$-doped lead phosphate glasses and the effect of gamma irradiation. *Radiation Effects and Defects in Solids*. 2012;167(4):256-267.

20. Ramachandra Rao MV, Gandhi Y, Srinivasa Rao L, Sahayabaskaran G, Veeraiah N. Electrical and spectroscopic properties of LiF–Bi$_2$O$_3$–P$_2$O$_5$:TiO$_2$ glass system. *Materials Chemistry and Physics*. 2011;126(1-2):58-68.

21. Sene FF, Martinelli JR, Gomes L. Synthesis and characterization of niobium phosphate glasses containing barium and potassium. *Journal of Non-Crystalline Solids*. 2004;348:30-37.